Extended Abstract #194
18th International Colloquium on the Dynamics of Explosions and Reactive Systems
Seattle, Washington, July 29–August 3, 2001

Higher-Order Conditional Moment Closure Modeling of Turbulent Nonpremixed Combustion

Chong Cha
chongcha@stanford.edu

Heinz Pitsch
h.pitsch@stanford.edu

Center for Turbulence Research
Stanford University
Stanford, CA 94305-3030
USA

Currently, a fundamental closure approximation in singly-conditional moment closure modeling [1] of turbulent, nonpremixed combustion is first-order closure of the average nonlinear chemical source terms, $\dot{\boldsymbol{w}}$, conditioned on the mixture fraction, $\xi(t,\boldsymbol{x})$:

$$\langle \dot{\boldsymbol{w}}(\boldsymbol{Y}(t,\boldsymbol{x}),\theta(t,\boldsymbol{x}),\rho(t,\boldsymbol{x}))|\xi(t,\boldsymbol{x})\rangle \approx \dot{\boldsymbol{w}}(\langle \boldsymbol{Y}|\xi\rangle,\langle\theta|\xi\rangle,\langle\rho|\xi\rangle) \quad , \tag{1}$$

where $\boldsymbol{Y}$ is the vector of mass fractions of the reacting species, and θ and ρ are the suitably nondimensionalized temperature and density of the mixture, respectively. For convenience, the notation used presently does not distinguish between the random variable and its corresponding sample space variable. The utility of first-order closure using conditional averaging is illustrated in Fig. 1, which shows in subplot (i) the reduced temperature θ as a function of ξ from the direct numerical simulation (DNS) experiment of Sripakagorn *et al.* [2]. Subplot (ii) shows the probability density function (pdf) of θ conditioned on ξ within a given range of $\xi_{\rm st} \pm \Delta\xi$, where $\xi_{\rm st}$ is the stoichiometric value of the mixture fraction, 0.5 for this case. $\Delta\xi$ decreases from the dash-dot line to the dash-dash line and finally to $\Delta\xi \approx 0$ for the solid line. Thus, the solid line is a representation of the conditional pdf of θ at $\xi_{\rm st}$. The figure illustrates three points: (i) The inapplicability of first-moment closure under conventional (unconditional) averaging, as is well known; (ii) the much improved representation of the pdf of θ by its mean value alone due to conditioning on ξ, helping to validate Eq. (1); and (iii) a negative skewness of the pdf due to the existence of local extinction and reignition events in this (numerical) experiment which threatens the validity of Eq. (1). The extinction/reignition events, clearly visible in subplot (i) and evident in the pdfs at low values of $\theta_{\rm st}$ in subplot (ii), are interpreted as fluctuations about the singly-conditional mean in a singly-conditional moment closure modeling framework.

Recently, modeling of the variance has been proposed to improve closure of the singly-conditional chemical source term [3–5]. Presently, we investigate the feasibility of higher-order closure (up to third-order) under singly-conditional moments. The DNS experiment of Sripakagorn *et al.* [2], specifically designed to investigate extinction/reignition, offers an ideal test-case to investigate the merits and drawbacks of higher-order closure strategies in a conditional moment closure modeling framework.

The production rates for fuel (F), oxidizer (O), and product (P) for the present numerical experiment of F + O $\rightleftharpoons$ 2P evolving in isotropic, homogeneous, and decaying turbulence are $\dot{w}_{\rm F} = -\dot{w}$, $\dot{w}_{\rm O} = -\dot{w}$, and $\dot{w}_{\rm P} = 2\dot{w}$, respectively, where

$$\dot{w}(Y_{\rm F},Y_{\rm O},Y_{\rm P},\theta) = A\exp\left(-\frac{\rm Ze}{\alpha}\right)\left(Y_{\rm F}Y_{\rm O}-\frac{1}{K}Y_{\rm P}^2\right)\exp\left[-\frac{\rm Ze(1-\theta)}{1-\alpha(1-\theta)}\right] \tag{2}$$

is the reaction-rate. Here, A is the frequency factor (multiplied by density and divided by molecular weight, assumed equal for all species), α is the heat release parameter, and Ze is the Zeldovich number. The Schmidt number is 0.7 and Lewis numbers are unity. The turbulent flow is incompressible and the molecular diffusivities and viscosity are independent of the temperature (*cf.* Sripakagorn [2] for details of the simulation).

The singly-conditioned average of $\dot{w}$ as a function of all singly-conditional moments can be obtained with: (i) A series expansion of the second exponential in Eq. (2) about $\epsilon \equiv \alpha\theta'/(1-\alpha(1-\langle\theta|\xi\rangle))$, where $\theta' \equiv \theta - \langle\theta|\xi\rangle$, valid for $|\epsilon| < \infty$; (ii) a series expansion for $(1+\epsilon)^{-1}$, valid for $|\epsilon| < 1$; and (iii) a decomposition of all species

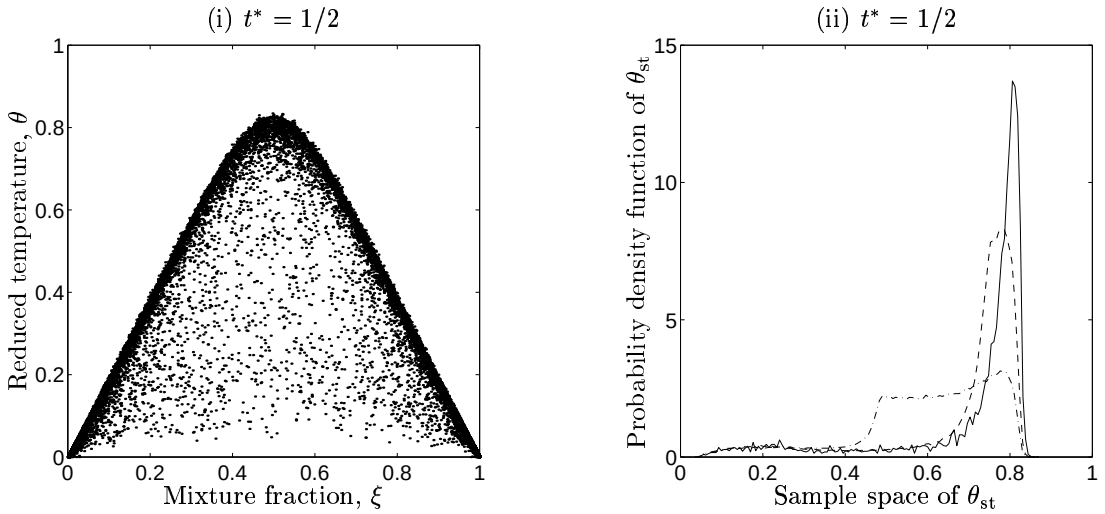

FIGURE 1: Motivation of the work. Subplot (i) is a scatter plot of the reduced temperature, θ, as a function of the local mixture fraction, ξ, at $t^* = 1/2$ (time has been nondimensionalized by the initial large-eddy turnover time) from the direct numerical simulation (DNS) experiment of Sripakagorn *et al.* [2]. (In the DNS, F + O $\leftrightarrow$ 2P evolves in decaying, homogeneous, isotropic turbulence with an initial $\mathrm{Re}_\lambda = 33$ on a 128^3 grid.) Subplot (ii) shows the conditional probability density function (pdf) of θ conditioned on ξ within a decreasing range of ξ values about $\xi_{\rm st} = 0.5$, the stoichiometric value of the mixture fraction: The range decreases from the dash-dot line to the dash-dash line and finally to the pdf conditioned on $\xi \approx \xi_{\rm st}$.

mass fractions about their singly-conditional means, $Y = \langle Y|\xi\rangle + Y'$. Singly-conditional averaging the result yields for the forward reaction-rate

$$\begin{aligned}
\langle \dot{w}(Y_{\rm F}, Y_{\rm O}, Y_{\rm P}, \theta)|\xi\rangle &= \dot{w}(\langle Y_{\rm F}|\xi\rangle, \langle Y_{\rm O}|\xi\rangle, \langle Y_{\rm P}|\xi\rangle, \langle\theta|\xi\rangle)(1 + B' + C' + \text{H.O.T.}) \qquad (3)\\
B' &= \frac{\langle Y'_{\rm F} Y'_{\rm O}|\xi\rangle}{\langle Y_{\rm F}|\xi\rangle\langle Y'_{\rm O}|\xi\rangle} + \frac{\beta}{[1-\alpha(1-\langle\theta|\xi\rangle)]^2}\left(\frac{\langle Y'_{\rm F}\theta'|\xi\rangle}{\langle Y_{\rm F}|\xi\rangle} + \frac{\langle Y'_{\rm O}\theta'|\xi\rangle}{\langle Y_{\rm O}|\xi\rangle}\right)\\
&\quad + \left(\frac{\beta/2}{1-\alpha(1-\langle\theta|\xi\rangle)} - \alpha\right)\frac{\langle\theta'^2|\xi\rangle}{[1-\alpha(1-\langle\theta|\xi\rangle)]^3}\\
C' &= \left(\frac{\beta/2}{1-\alpha(1-\langle\theta|\xi\rangle)} - \alpha\right)\frac{\alpha^2/\beta}{1-\alpha(1-\langle\theta|\xi\rangle)}\left(\frac{\langle Y'_{\rm F}\theta'^2|\xi\rangle}{\langle Y_{\rm F}|\xi\rangle} + \frac{\langle Y'_{\rm O}\theta'^2|\xi\rangle}{\langle Y_{\rm O}|\xi\rangle}\right)\\
&\quad + \frac{\alpha}{1-\alpha(1-\langle\theta|\xi\rangle)}\frac{\langle Y'_{\rm F}Y'_{\rm O}\theta'|\xi\rangle}{\langle Y_{\rm F}|\xi\rangle\langle Y_{\rm O}|\xi\rangle} - \frac{\alpha^4/\beta}{[1-\alpha(1-\langle\theta|\xi\rangle)]^2}\langle\theta'^3|\xi\rangle
\end{aligned}$$

valid for $|\epsilon| < 1$. The complete series is always convergent for $\alpha \leq 1$. For the present case of a single-step reaction, the conditional averages of all species and temperature can be obtained from the single equation for the average of θ singly-conditioned on ξ:

$$\frac{d}{dt}\langle\theta|\xi\rangle = \frac{\langle\chi|\xi\rangle}{2}\frac{\partial^2}{\partial\eta^2}\langle\theta|\xi\rangle + 2\dot{w}(\langle Y_{\rm F}|\xi\rangle, \langle Y_{\rm O}|\xi\rangle, \langle Y_{\rm P}|\xi\rangle, \langle\theta|\xi\rangle)(1 + B + C) \ , \qquad (4)$$

where B and C also contain the contributions of the backward reaction. $\langle\chi|\xi\rangle$ is the conditionally-averaged scalar dissipation rate, specified directly from the DNS. e_Q and e_y closure has been invoked [6]. For convenience, Eq. (4) is referred to as the `cmc3` model (third-order closure), as the `cmc2` model with $C = 0$ (second-order closure), and as the `cmc1` model with both $B = 0$ and $C = 0$ (first-order closure). All double and triple conditional correlations are taken from the DNS.

Figure 2 compares the modeling results (lines) to the DNS experimental data (symbols). Solid circles are the singly-conditionally averaged temperature at $\xi_{\rm st}$ taken directly from the experiment. Subplot (i) is from the same case that was shown in Fig. 1. The deviation of $\langle\theta|\xi_{\rm st}\rangle$ from the equilibrium value, $\theta_{\rm eq} = 0.83$

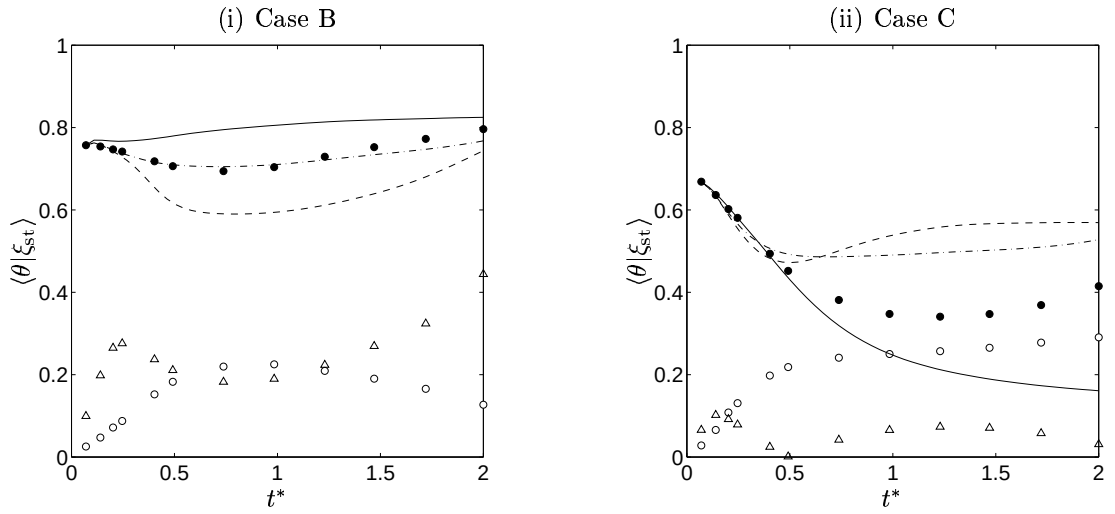

FIGURE 2: Comparison of modeling results with DNS data. Solid circles = singly-conditional average of the reduced temperature, $\langle\theta|\xi_{st}\rangle$, open circles = standard deviation about singly-conditional means, $(\langle\theta'^2|\xi_{st}\rangle)^{1/2}$, open triangles = skewness, $|s|/10$. Solid line = first-order, singly-conditional moment closure results (`cmc1`), dash-dash line = second-order modeling results (`cmc2`), and dash-dot line = third-order predictions (`cmc3`). Subplot (i) = moderate extinction case ("Case B") and subplot (ii) = high extinction case ("Case C") from Cha et al. [6].

at ξ_{st}, is due to the local extinction/reignition events that were seen in Fig. 1 (i). Only the frequency factor was decreased in the DNS for the case shown in Fig. 2 (ii), which results in increased extinction levels, and hence shows a larger deviation from θ_{eq} as compared to the case in subplot (i). (Subplots (i) and (ii) in Fig. 2 correspond to Cases B and C in [6].) Open circles are the standard deviation about $\langle\theta|\xi_{st}\rangle$ and open triangles are the (nondimensional) skewness defined as

$$s = \frac{1}{\langle\theta'^2|\xi\rangle^{3/2}} \int (\theta - \langle\theta|\xi\rangle)^3 p(\theta|\xi) d\theta \ ,$$

where $p(\theta|\xi)$ is the conditional pdf. Note that s is a function of $\langle\theta^3|\xi\rangle$, a third-order term. In Fig. 2, solid lines are first-order modeling results (`cmc1`), dash-dash lines are second-order predictions (`cmc2`), and dash-dot lines are third-order modeling results (`cmc3`).

In Case B (subplot (i) in Fig. 2), second-order closure causes the mean to be underpredicted. Consideration up to the third-order terms in Eq. (4) evidently counteracts this effect and leads to excellent predictions of the data.

In Case C (subplot (ii) in Fig. 2), first-order closure is unable to predict the onset of reignition (in the mean). Both second- and third-order closures can predict the global reignition, but deviates from the data beyond $t^* \gtrsim 1/2$. Of note is that the skewness, $|s|$, decreases in the higher extinction case while the variance remains comparable.

Discussion of the modeling results in Fig. 2 center around the conditional pdfs of θ at ξ_{st}, $p(\theta|\xi_{st})$, for representative times of interest. Figure 3 (left column) shows $p(\theta|\xi_{st})$ at $t^* = 1/4$, $1/2$, $3/4$, and $3/2$ for Case B. At early times ($t^* < 1/2$), the pdfs are unimodal—have a well-defined, single peak—with some negative skewness. The series expansion of the conditionally-averaged reaction rate, Eq. (3), does not know the shape of the pdf. Evidently, skewness, or third-order information, and variance, or second-order information, is sufficient to correct first-moment closure, resulting in the good agreement with the data that was seen in Fig. 2 (i). For larger times, $t^* \geq 1/2$, some bimodality begins to appear in the pdfs, but not enough to cause problems for third-order closure, the `cmc3` model. For a general unimodal pdf, at least third-order moments are required to capture skewness. For this experimental case with moderate local extinction levels, the skewness is always negative for $p(\theta|\xi_{st})$ as the temperature can never exceed θ_{eq}. The implication is that in such a circumstance at least third-order information is required in the series expansion of $\langle\dot{w}|\xi\rangle$.

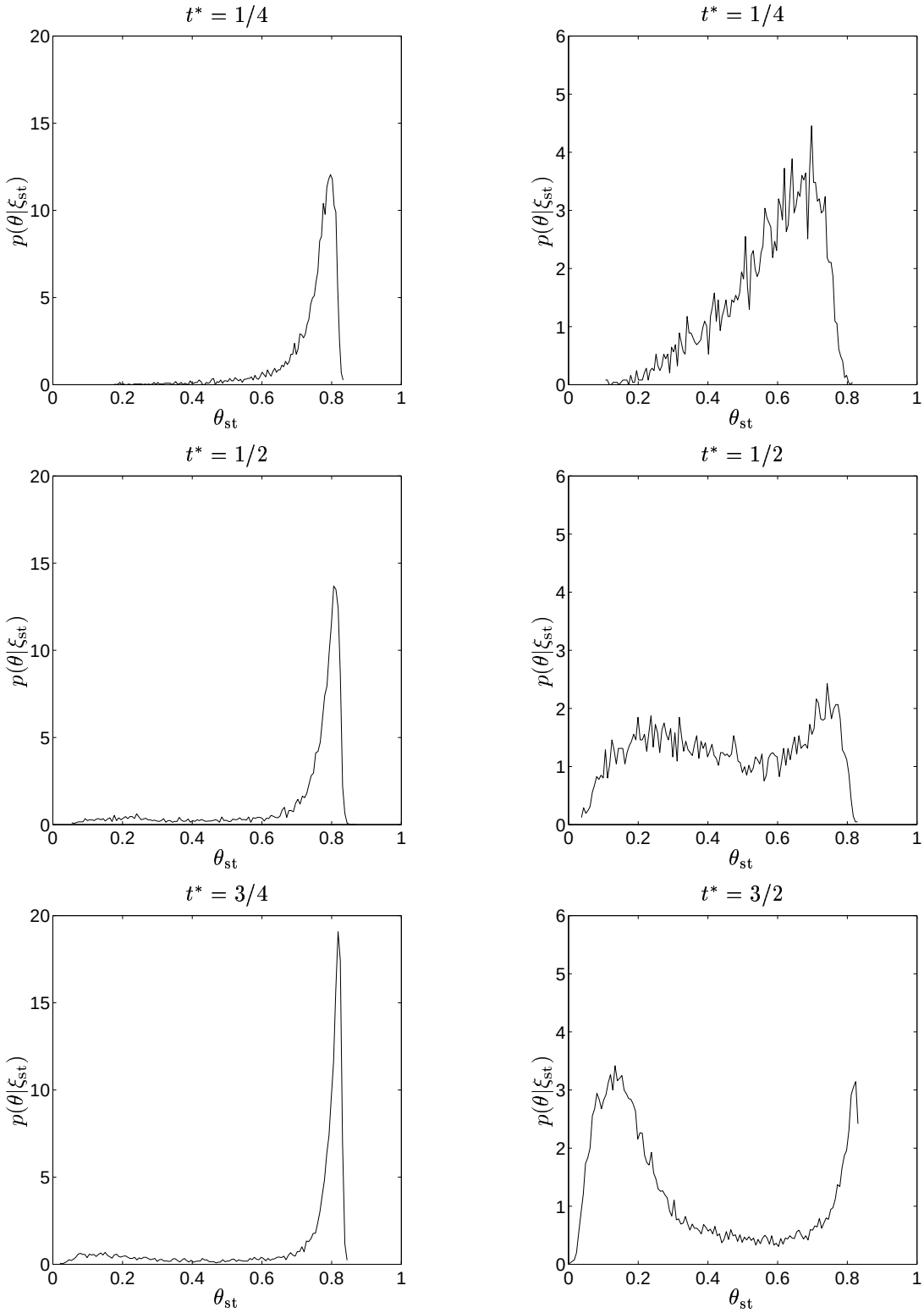

FIGURE 3: Conditional pdfs of θ at $\xi_{\rm st}$, $p(\theta|\xi_{\rm st})$ for Case B (left column) and Case C (right column).

Figure 3 (right column) shows $p(\theta|\xi_{\rm st})$ for Case C (corresponding to subplot (ii) in Fig. 2) at $t^* = 1/4$, 1/2, 3/4, and 3/2. For $t^* \lesssim 1/4$, the standard deviation about the conditional average is comparable to Case B, but with reduced skewness (*cf.* Fig. 2), and second-order closure yields comparable results to the third-order closure predictions. For $t^* \gtrsim 1/2$, the pdfs become bimodal—have well-defined, double peaks—and thus the skewness can no longer characterize the shape of the pdfs. Third-order closure also breaks-down. Bimodality becomes stronger for increasing times with comparable peak temperatures. The comparable standard deviations from the conditional mean for this case as compared to Case B (*cf.* Fig. 2) is due to the combined effect of the high extinction levels in this case, which decrease $\langle\theta|\xi_{\rm st}\rangle$, and the bimodality of the pdf. The cause of the reduction in the skewness from Case B is due to the remarkable symmetry in the pdfs. This persistence of symmetry of the bimodal pdfs could readily be exploited in future modeling efforts where the presumed bimodal shape of the conditional pdfs of θ could be characterized with only first- and second-moment information.

In summary, with moderate levels of local extinction, the conditional pdfs are unimodal (single peaked). Mean and variance information alone in the series expansion of the singly-conditional average of the chemical source term is insufficient to describe the influence of the fluctuations. That is, first- and second-order closure cannot describe the singly-conditional means and third-moments (or the skewness of the pdfs) are also required to obtain good predictions. With high levels of local extinction, the pdf can adopt a strong bimodal structure with little change in the twin peak locations. Third-order closure breaks-down. The persistence of the bimodality of the pdfs with extinction/reignition events suggests a strong possibility to model the chemical source term with only mean and variance information and a presumed, bimodal pdf shape.

Acknowledgements

The authors express gratitude to Paiboon Sripakagorn for making available to us his DNS database before publication.

References

[1] A. Yu. Klimenko and R. W. Bilger. Conditional moment closure for turbulent combustion. *Prog. Energy Combust. Sci.*, 25:595–687, 1999.

[2] Paiboon Sripakagorn, George Kosály, and Heinz Pitsch. Local extinction-reignition in turbulent non-premixed combustion. In *CTR Annual Research Briefs*, pages 117–128, Stanford University, 2000. Center for Turbulence Research.

[3] N. Swaminathan and R. W. Bilger. Conditional variance equation and its analysis. In *Twenty-Seventh Symposium (International) on Combustion*, pages 1191–1198, Pittsburgh, 1998. The Combustion Institute.

[4] A. Kronenburg, R. W. Bilger, and J. H. Kent. Second-order conditional moment closure for turbulent jet diffusion flames. In *Twenty-Seventh Symposium (International) on Combustion*, pages 1097–1104. The Combustion Institute, 1998.

[5] E. Mastorakos and R. W. Bilger. Second-order conditional moment closure for the autoignition of turbulent flows. *Phys. Fluids*, 10(6):1246–1248, 1998.

[6] C. M. Cha, G. Kosály, and H. Pitsch. Modeling extinction and reignition in turbulent nonpremixed combustion using a doubly-conditional moment closure approach. *Phys. Fluids*, submitted.